PERGAMON

Building and Environment 36 (2001) 543–559

BUILDING AND ENVIRONMENT

www.elsevier.com/locate/buildenv

On the simulation of the plume from stacks of buildings

Seyhan Uygur Onbaşıoğlu

Mechanical Engineering Department, Istanbul Technical University, 80191, Gumussuyu, Istanbul, Turkey

Received 23 April 1998; received in revised form 25 November 1998; accepted 7 February 2000

Abstract

A three-dimensional numerical model is used for a turbulent buoyant jet. The standard k–ϵ model has been modified to focus on the buoyancy-production term. The usual and modified buoyancy production coefficients are used for comparisons with experimental data reported in the literature. Imported numerical results are obtained with the modified coefficient for the stack-exit velocities and temperatures. The effects of these parameters on flow characteristics are discussed. © 2000 Elsevier Science Ltd. All rights reserved.

1. Introduction

Turbulent mixing of a buoyant jet in a cross flow is a serious problem. The plume from stacks of buildings typically discharge pollutants into the atmosphere. Avoiding pollutant dispersions near air-conditioning intakes is an important goal in plume control. When the flow is driven by the source momentum flux, it is referred to as a heated jet. When the flow is driven by buoyancy flux, it is referred to as a plume.

The integral method used in plume simulation involves the use of the temperature distribution as a factor in plume rise [1]. However, wind-tunnel simulation experiments only include parameters such as stack height, exhaust speed and wind direction [2–4]. Differential method, on the other hand, needs employment of a turbulence model, this is why the differential method has been developed simultaneously with the turbulence modeling.

The most important problem in these studies is the significant anisotropy of the turbulence as a consequence of buoyancy. Investigations using a parabolic set of equations [5] and algebraic stress models [6] are present in literature. The former has some restrictions and the algebraic or Reynolds stress models need an enormous computing time and memory. Also, a standard k–ϵ model is used to simulate the turbulent phenomena [7]. In spite of the model's reasonable computing requirements, it may be concluded that the use of k–ϵ theory in such a flow is not appropriate. In the present work, standard k–ϵ model is modified to focus on the coefficient in the context of buoyancy production term to optimize the model for a reasonable computing time and space requirement and well representation of buoyancy. Experiments to obtain comprehensive turbulence data to test and improve turbulence models are available [8]. Comparisons with the experimental data and comparisons between different numerical solutions [7–9] are used to demonstrate the quality of the simulation.

2. Modeling the flow

A three-dimensional flow field of a buoyant jet exiting from a square stack of dimension D has been considered. The jet has constant injection velocity V_e, issuing vertically into a uniform-velocity cross flow of non-stratified fluid. Fig. 1 shows the geometry and coordinates of the flow problem.

With the assumption that the Boussinessq approximation is valid, the following governing equations are obtained:

- continuity

PII: S0360-1323(00)00021-4

Nomenclature

B	body force per unit volume (N/m^3)
C	concentration (kg pollutant/kg air)
D	stack diameter (m)
Fr	Froude number, $V_e^2/g\beta(\Delta T)D$
g_i	gravitational acceleration (m/s^2)
G_k	buoyancy production (m^2/s^3)
k	turbulence kinetic energy (m^2/s^2)
P	pressure (Pa)
P_k	shear stress production (m^2/s^3)
S_ϕ	source term of the general equation
t	time (s)
T	temperature (K)
U_a	ambient velocity (m/s)
u	horizontal velocity (m/s)
u_i'	fluctuate velocity (m/s)
V	vertical velocity (m/s)
V_e	exit velocity (m/s)

Greek symbols

β	volume expansivity ($1/K$)
ϵ	dissipation of turbulence kinetic energy (m^2/s^3)
ϕ	dependent variable
μ	dynamic viscosity (kg/ms)
μ_t	turbulent dynamic viscosity (kg/ms)
ν	kinematic viscosity (m^2/s)
ν_t	turbulent kinematic viscosity (m^2/s)
ρ	density (kg/m^3)
σ_k, σ_ϵ	empirical diffusion constants
σ_t	turbulent Prandtl number
σ_{Sc}	turbulent Schmidt number

Subscripts

a	ambient
e	exit
i,j	tensor index

$$\rho\frac{\partial(U_i)}{\partial x_i}=0 \tag{1}$$

- momentum

$$\rho\frac{\partial U_i}{\partial t}+\rho U_j\frac{\partial U_i}{\partial x_j}=\frac{\partial}{\partial x_j}\left[\mu\frac{\partial U_i}{\partial x_j}-\rho\overline{u_iu_j}\right]-\frac{\partial P}{\partial x_i}+B \tag{2}$$

where the body forces due to temperature differences are

$$B=\rho g_i\beta(T_e-T)$$

- energy

$$\frac{\partial T}{\partial t}+U_j\frac{\partial T}{\partial x_j}=\frac{\partial}{\partial x_j}\left[\frac{\nu}{Pr}\frac{\partial T}{\partial x_j}-\overline{u_iT'}\right]$$

- concentration of pollutant

$$\frac{\partial C}{\partial t}+U_j\frac{\partial C}{\partial x_j}=\frac{\partial}{\partial x_j}=\left[\frac{\nu}{Sc}\frac{\partial C}{\partial x_j}-\overline{u_iC'}\right].$$

We employ an isotropic eddy viscosity and eddy fusivity, i.e. the eddy viscosities and diffusivities the same for all Reynolds-stress components and sc fluxes, viz.,

$$-\overline{u_iu_j}=\nu_t\left(\frac{\partial u_i}{\partial x_j}+\frac{\partial u_j}{\partial x_i}\right)-\frac{2}{3}k\delta_{ij}$$

$$-\overline{u_iT'}=\frac{\nu_t}{\sigma_t}\frac{\partial T}{\partial x_i}$$

$$-\overline{u_iC'}=\frac{\nu_t}{\sigma_c}\frac{\partial T}{\partial x_i}$$

where

$$\nu_t=c_\mu\frac{k^2}{\epsilon}$$

The equations that govern the distribution of k a are:

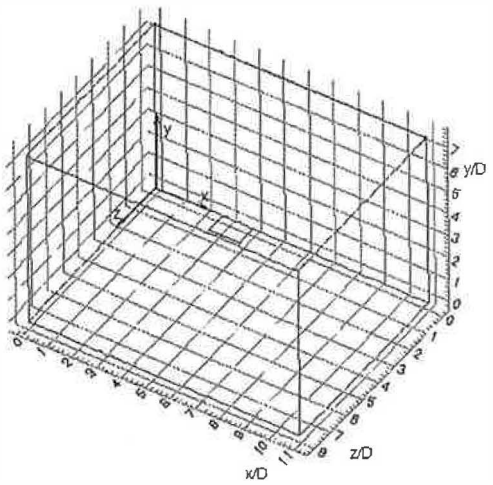

Fig. 1. The arrangement of the computational grid.

$$\frac{Dk}{Dt} = \frac{\partial}{\partial x_i}\left[\left(\frac{\nu_t}{\sigma_k} + \nu\right)\frac{\partial K}{\partial x_i}\right] + P_k + G_k + \epsilon \tag{9}$$

$$\frac{D\epsilon}{Dt} = \frac{\partial}{\partial x_i}\left[\left(\frac{\nu_t}{\sigma_\epsilon} + \nu\right)\frac{\partial \epsilon}{\partial x_i}\right] + c_{\epsilon 1}\frac{\epsilon}{k}(P_k + c_{\epsilon 3}G_k) - c_{\epsilon 2}\frac{\epsilon^2}{k} \tag{10}$$

where P_k is the shear stress production,

$$P_k = -\overline{u_i u_j}\frac{\partial U_i}{\partial x_j} \tag{11}$$

G_k is the buoyancy production term,

$$G_k = -g_i\beta\overline{u_i T'} \tag{12}$$

and σ_k and σ_ϵ are empirical diffusion constants.

Eqs. (9) and (10) are sensitive to the value of the coefficients. The coefficients adopted in this study are:

$$c_\mu = 0.09;\ c_1 = 1.44;\ c_2 = 1.92;\ c_{\epsilon 3} = 0.8;$$

$$\sigma_k = 1.0;\ \sigma_\epsilon = 1.3;\ \sigma_t = 0.7;\ \sigma_c = 0.6.$$

For non-buoyant flows, the buoyancy production term G_k is of no consequence. However, for a buoyant flow, the coefficient $c_{\epsilon 3}$ can have a significant effect. It is usually assumed that both the stress and buoyancy production rates should affect the level of dissipation in a similar manner. Thus, the value of $c_{\epsilon 3}$ is usually

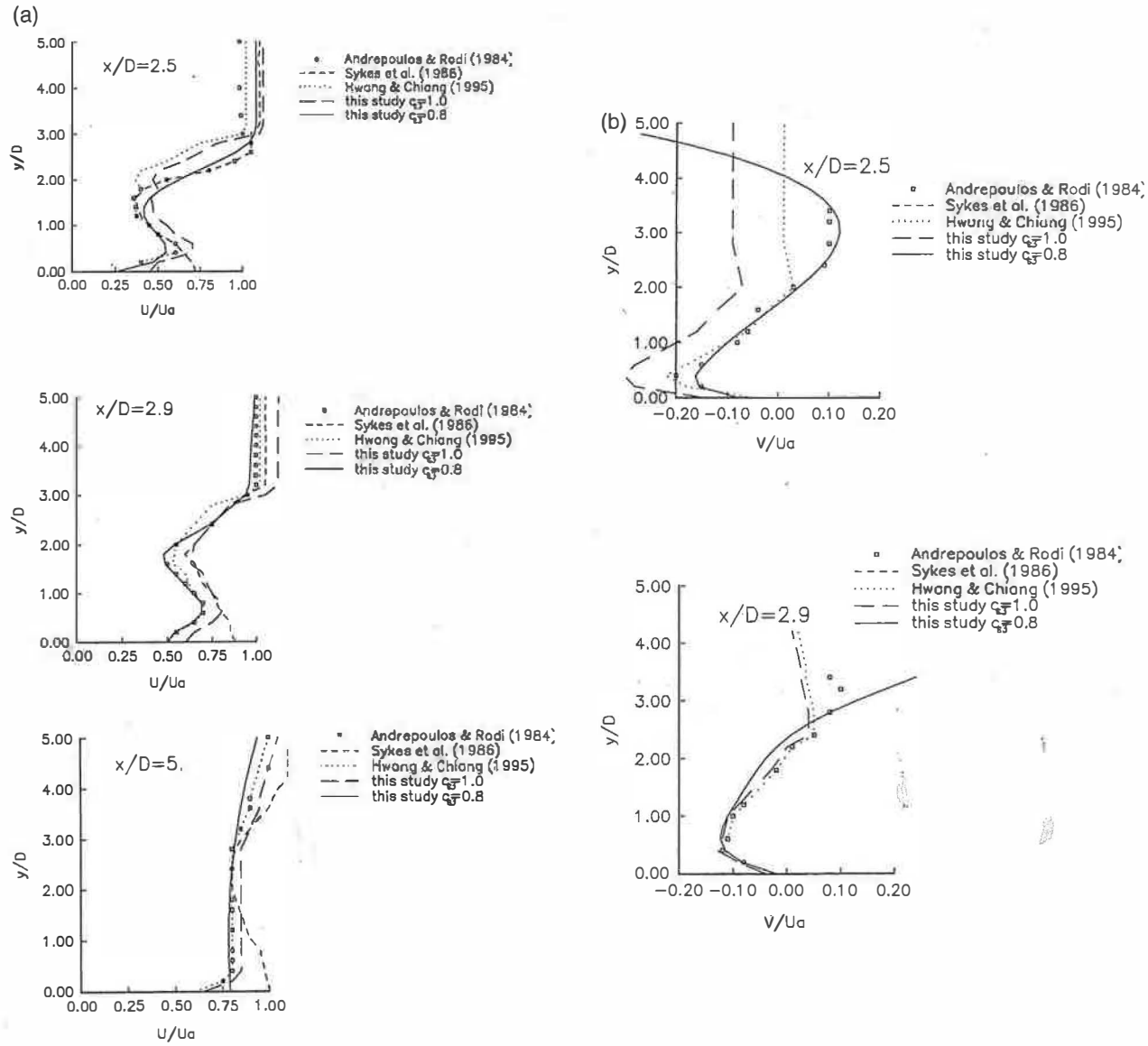

Fig. 2. Comparison of predicted profiles for $V_e/U_a = 2$ at the $z = 0$ plane with data reported from Refs [7–9].

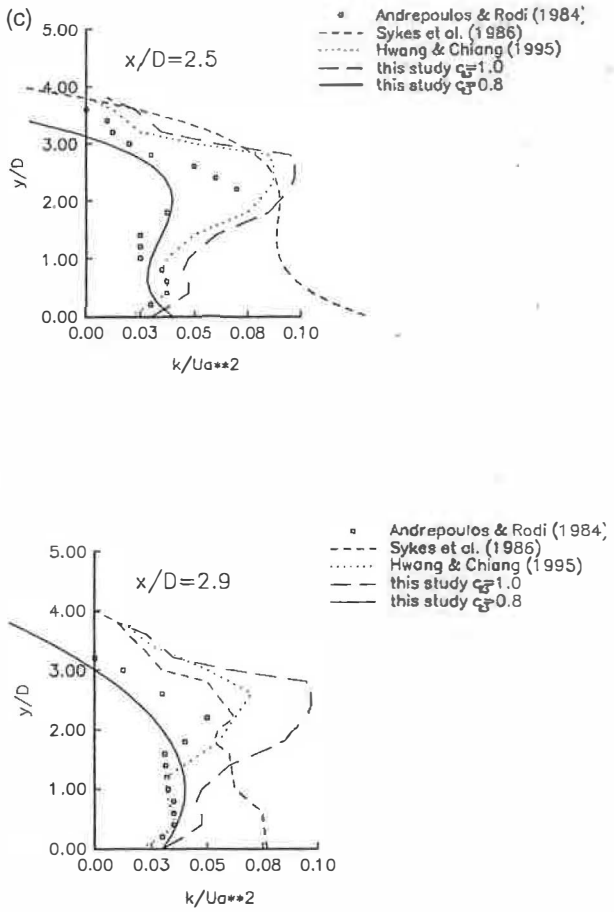

Fig. 2 (*continued*)

set equal to 1. The present study considers a value of $c_{\epsilon 3}=0.8$. To reduce the level of a buoyancy production term in dissipation equations, results in differences in consistency with the experimental data.

3. Computational technique

Computations are performed by discretization of the governing equations on a collocated grid arrangement, using the finite volume technique. Convection terms are formulated by a hybrid scheme and diffusion term

Table 1
The jet flow conditions and flow parameters under investigation

V_e/U_a	T_e (K)	Fr
1.00	600	0.16
2.00	600	0.65
4.50	600	3.31
8.00	600	13.22
8.00	450	24.55
18.0	600	52.89
8.00	275	∞

formulation is held by arithmetic mean option. T solution algorithm is the PISO (Pressure Implicit wi Splitting of Operations) scheme which is basically time marching procedure. Incomplete factorization f the pressure equation and Alternate Directions Impli (ADI) method for the other equations are used.

3.1. Boundary conditions

For the discharge of a buoyant jet into a non-stra fied fluid, it can be seen from Fig. 1 that the time-av aged flow field is symmetrical about the x–y pla passing through the center of the jet. The calculati domain in the z direction extends from the symme plane to $z/D = 7.5$. In the y direction, one boundary the bottom plane and the other is sufficiently far av so that uniform cross-stream conditions may assumed. This location was determined computati ally and was found to be at $y/D = 7.5$. In the x dir tion, the upstream boundary was placed 2.5 upstream of the jet and the position of the downstre boundary was located sufficiently far downstream that the flow velocity became almost parallel to th direction at $x/D = 11.0$. The boundaries for cal

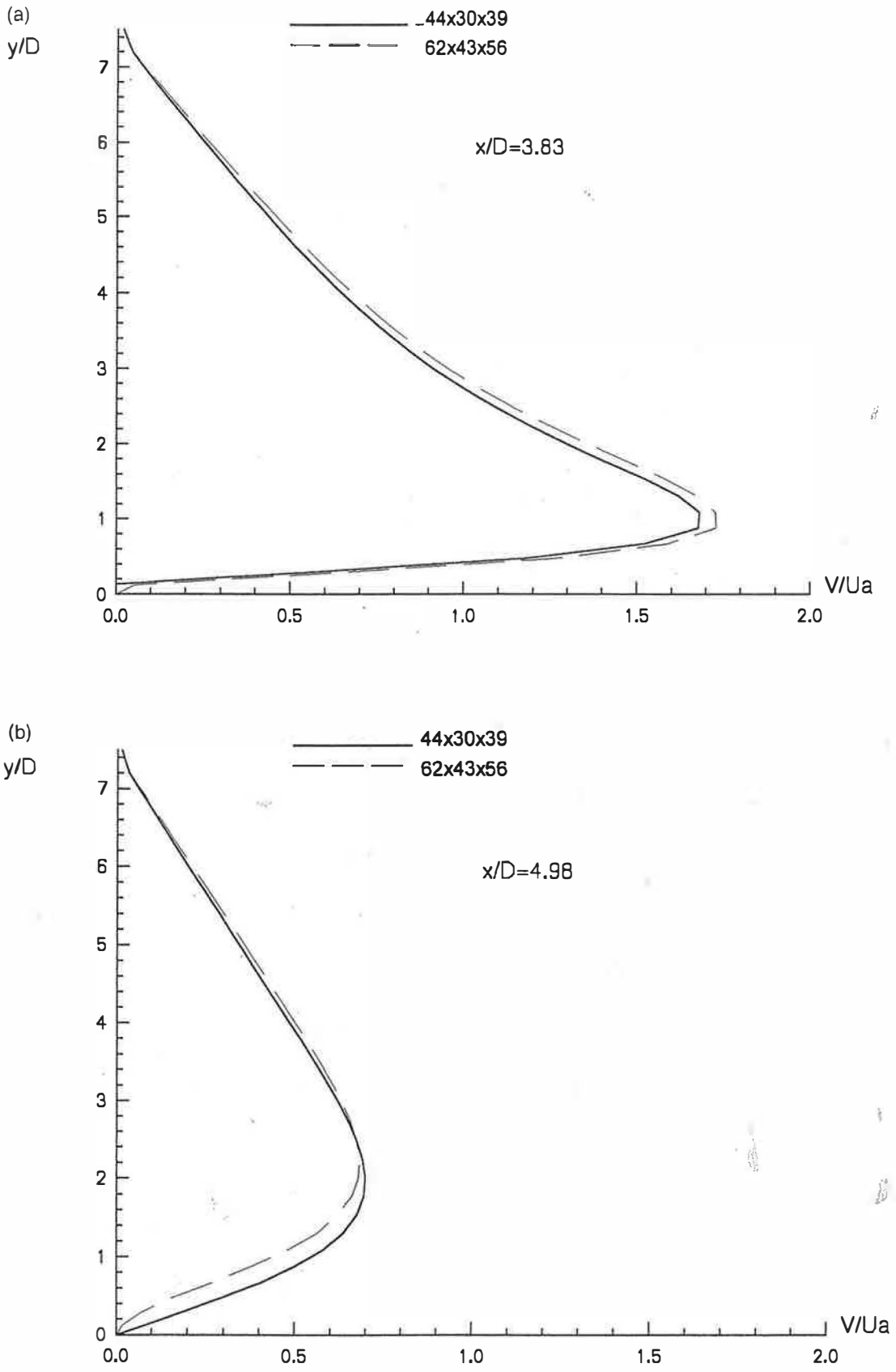

Fig. 3. Comparison of the predicted V profiles at $z = 0$ for $V_e/U = 8$ between two grid solutions $44 \times 30 \times 39$ and those of the fine grid $62 \times 43 \times 56$.

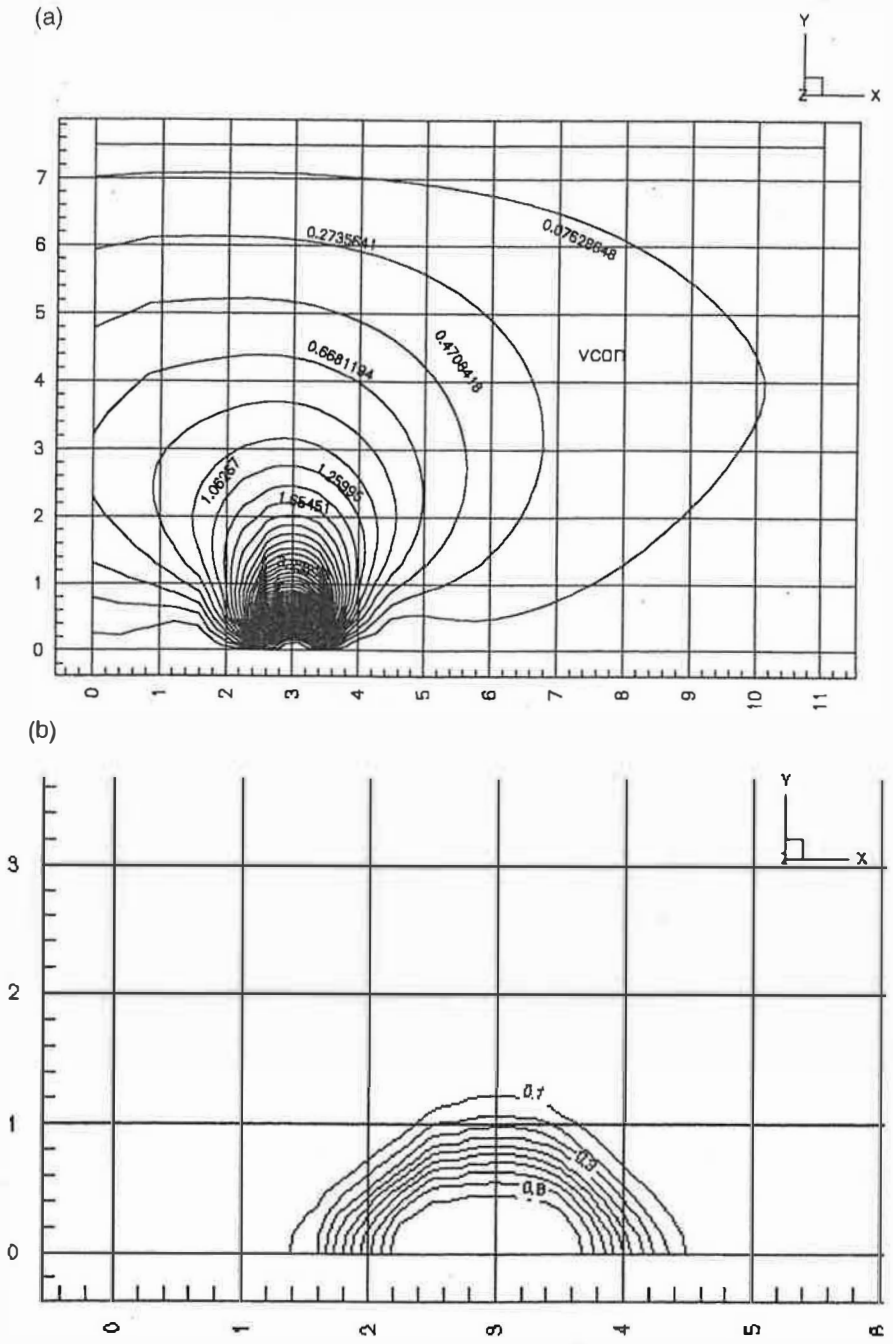

Fig. 4. (a) The vertical non-dimensional velocity contours (V_c/U_a) and (b) iso-concentration contours for $V_c/U = 8$ case.

lations then became $X_1 = 2.5\ D$, $X_2 = 11.0\ D$, $Y_1 = 7.5\ D$, $Z_1 = D/2$, $Z_2 = 8.0\ D$.

- Upstream boundary conditions

$x = 0; \quad 0 < y < Y_1; \quad 0 < z < Z_2.$

The flow was considered to be far removed from the jet with

$U = U_a; \quad V = W = C = 0; \quad T = T_a; \quad k = 0.04\ U$

$\epsilon = k^{3/2}/0.06 Y_1.$

- Downstream boundary conditions

$x = X_2; \quad 0 < y < Y_1; \quad 0 < z < Z_2.$

The normal gradients of the variables were assum

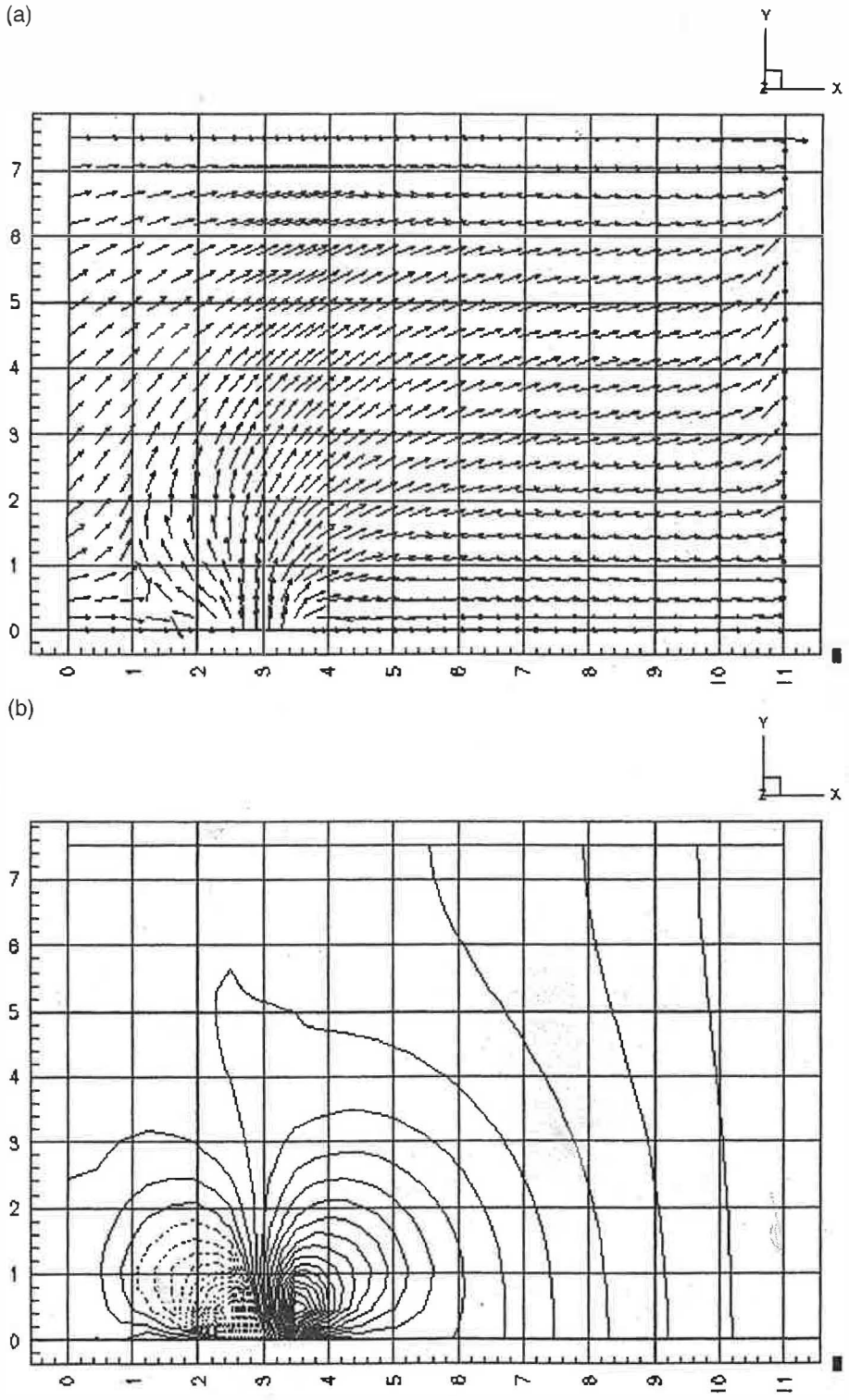

Fig. 5. The computed results on the $z = 0$ plane for $V_c/U = 18$. (a) The U–V velocity vectors. (b) The stream-wise velocity (U) contours (negative values are shown dashed).

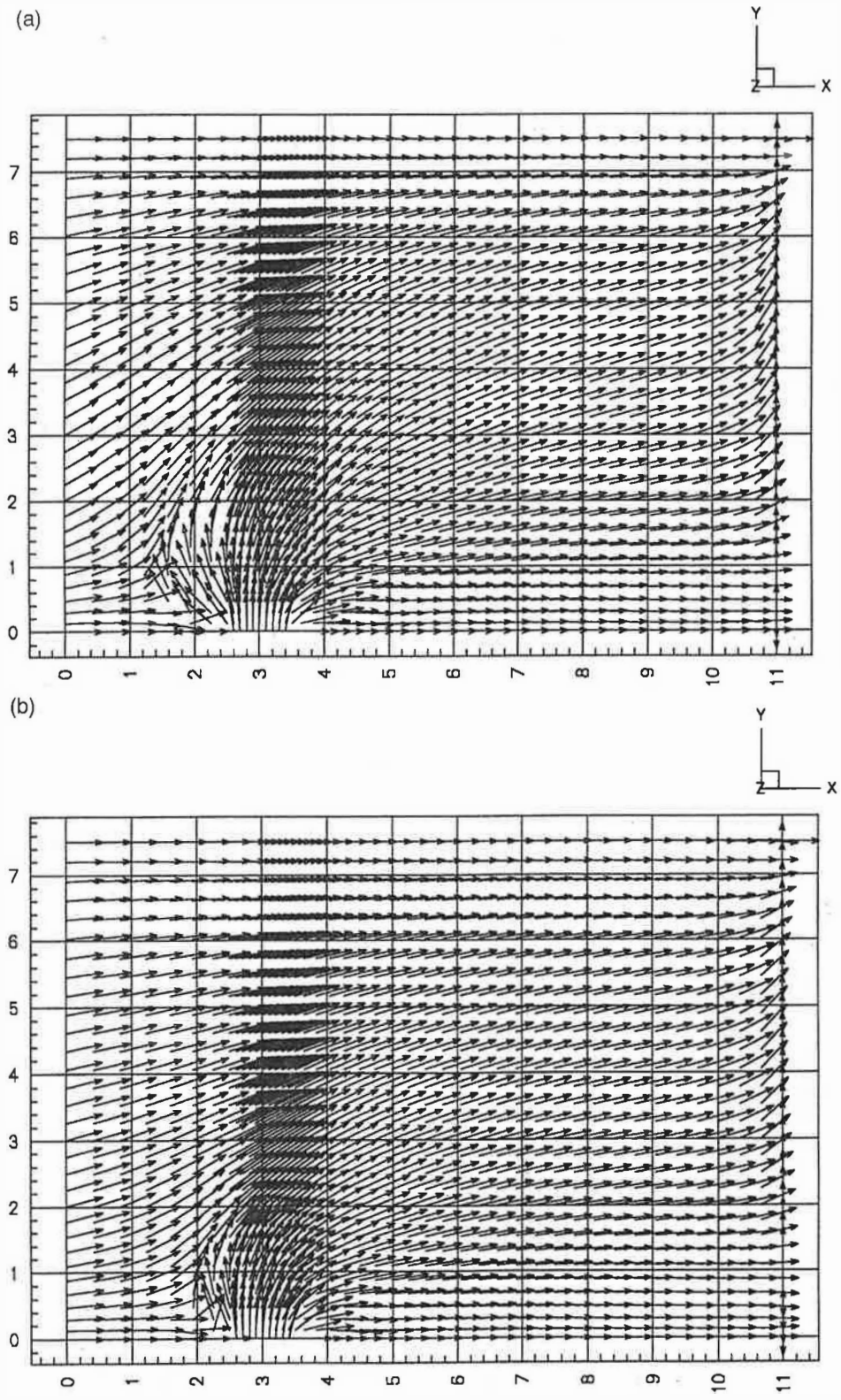

Fig. 6. Effect of jet exit velocity on plume rise: (a) $V_e/U = 8$ ($Fr = 13.22$); (b) $V_e/U = 4.5$ ($Fr = 3.31$); (c) $V_e/U = 2.0$ ($Fr = 0.65$); (d) $V_e/U =$ ($Fr = 0.16$).

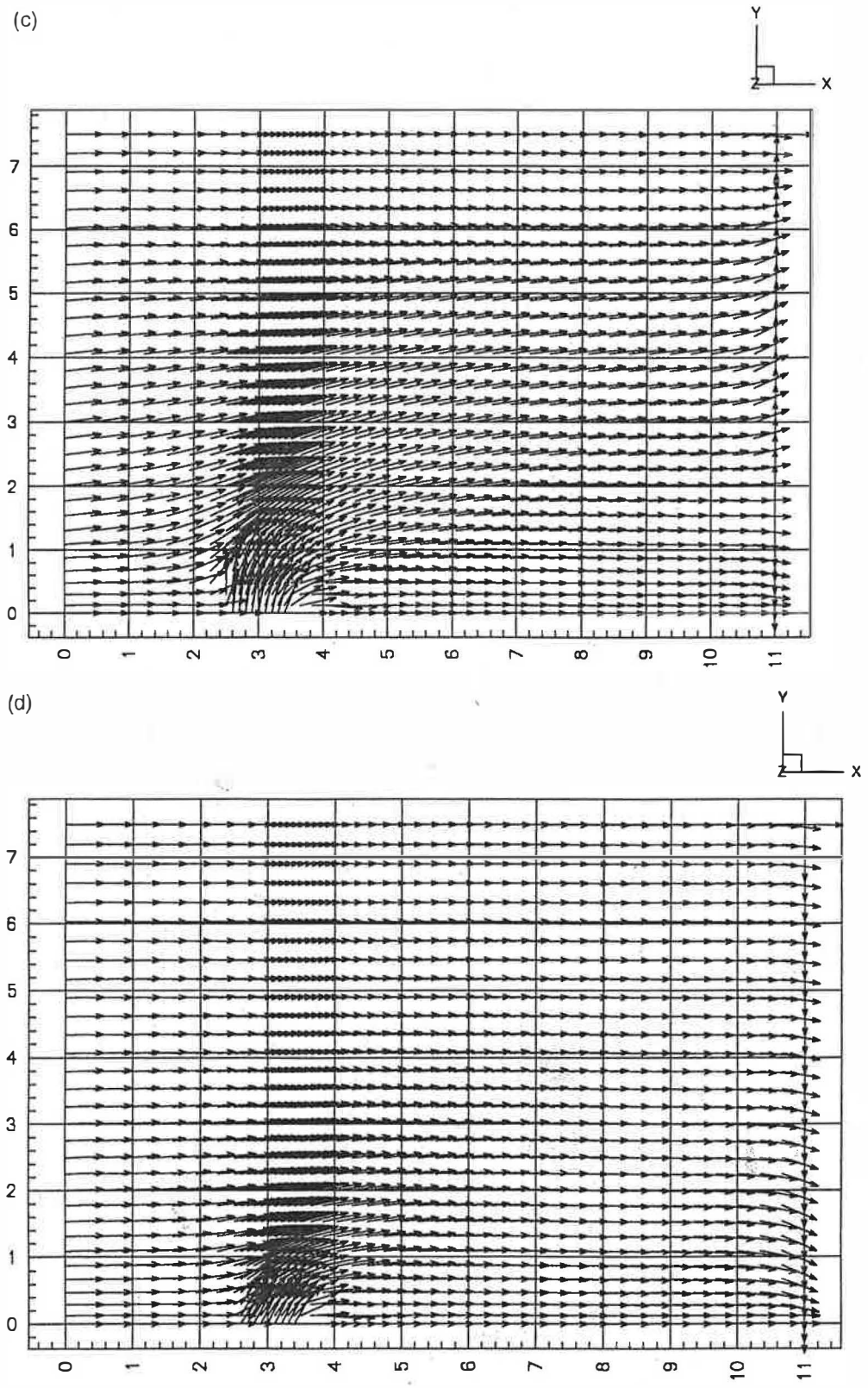

Fig. 6 (*continued*)

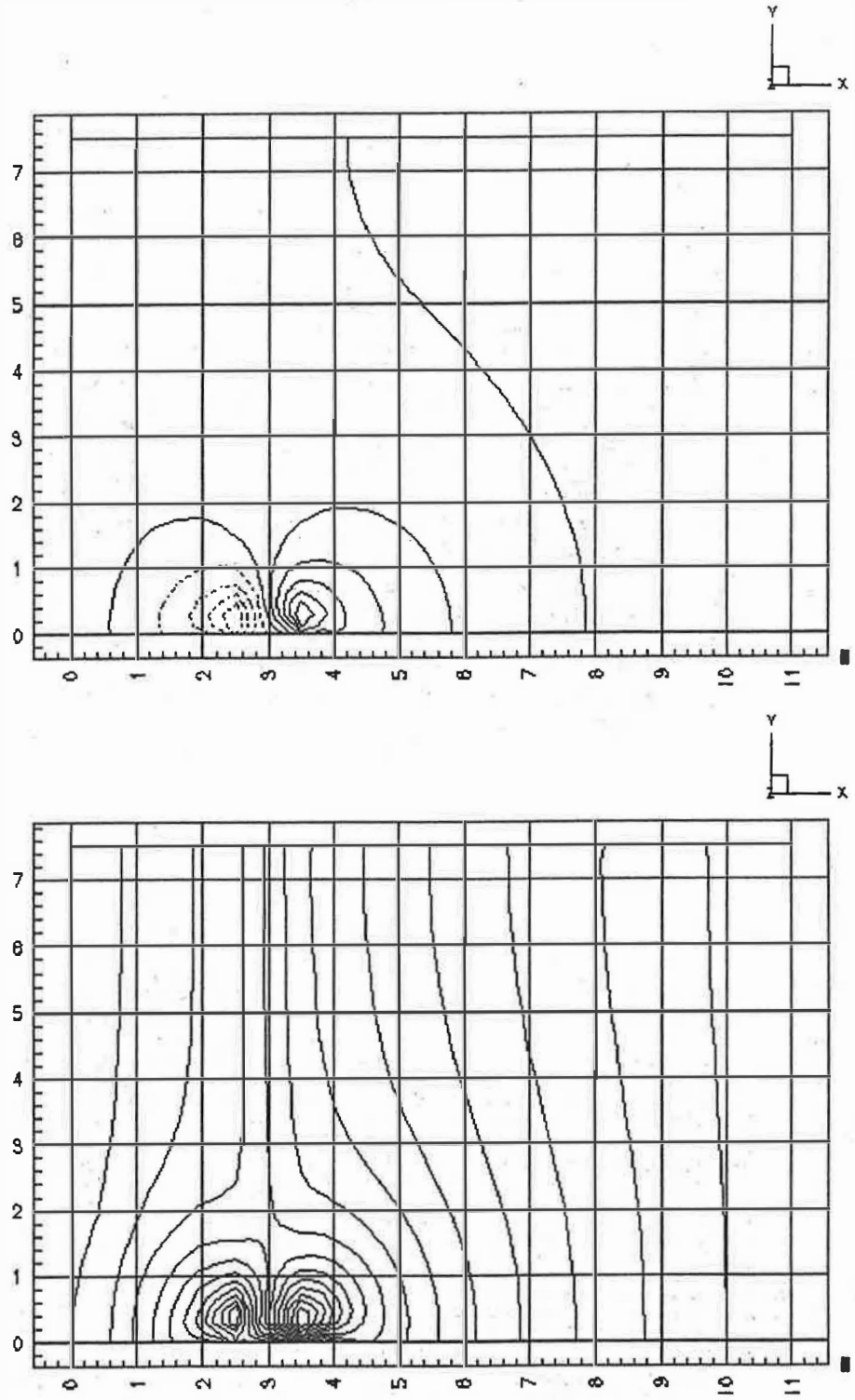

Fig. 7. The stream-wise velocity contours for: (a) $V_e/U = 4.5$ ($Fr = 0.65$); (b) $V_e/U = 2$ ($Fr = 0.16$) (negative values are shown dashed).

to be zero, i.e. $\partial(V, W, T, k, \epsilon, C)/\partial x = 0$; also, $U_B = U^n_{B-1}$ where n and B represent iteration level and boundary, respectively.

- Jet exit boundary conditions

$$X_1 < x < X_1 + D; \quad y = 0; \quad 0 < z < Z_1.$$

The conditions were specified as:

$$V = V_{\text{exit}}; \quad U = V = W = 0; \quad T = T_{\text{exit}}; \quad C = C_{\text{exi}}$$

$$k = 0.001 V^2_{\text{exit}}; \quad \epsilon = k^{3/2}/0.5D$$

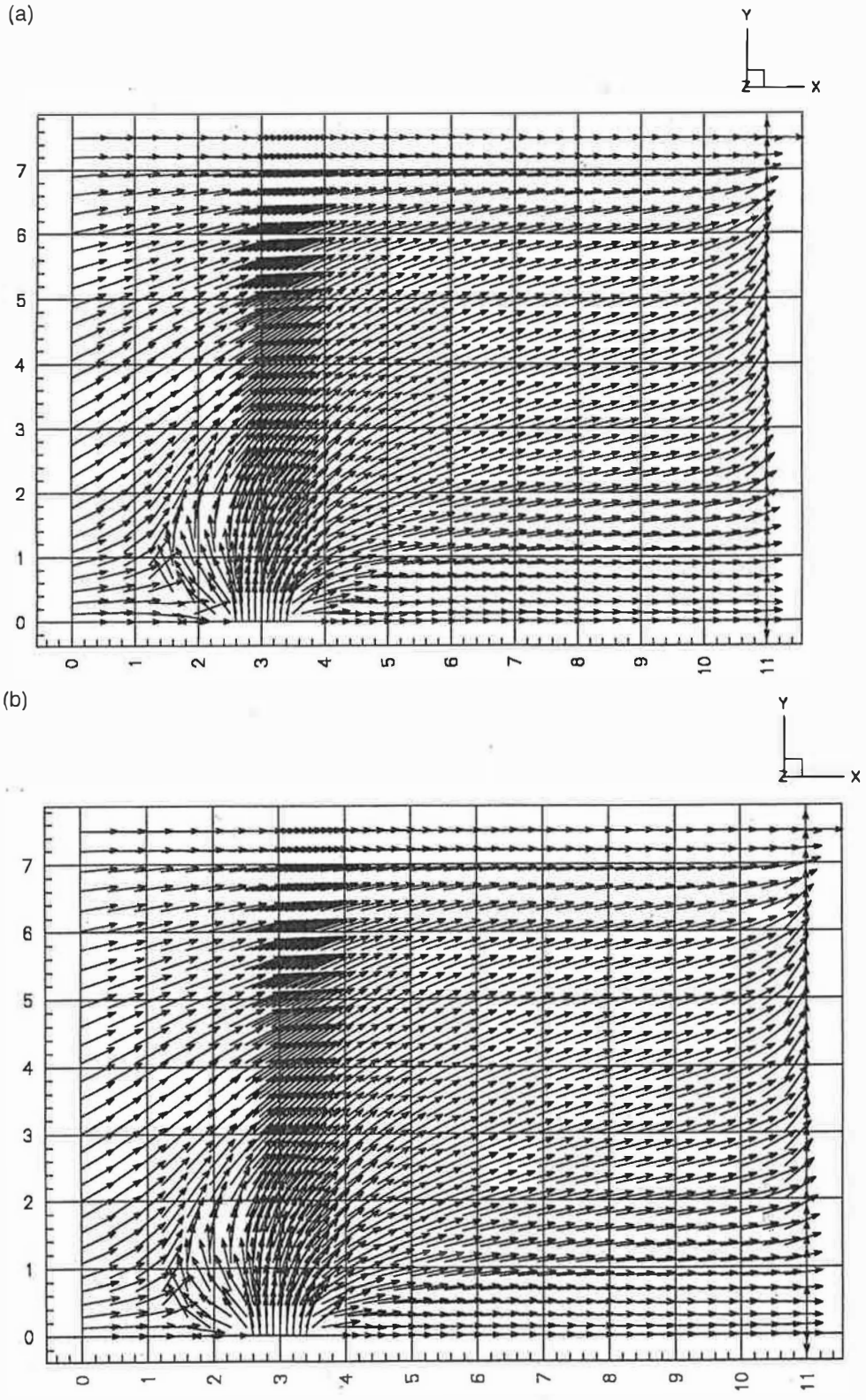

Fig. 8. Effect of the jet exit temperature on plume rise ($V_e/U = 8.0$). Velocity contours on the left and the streamlines on the right: (a) $T_e = 600$ K ($Fr = 13.22$); (b) $T_e = 450$ K ($Fr = 24.55$); (c) $T_e = 275$ K ($Fr = \infty$).

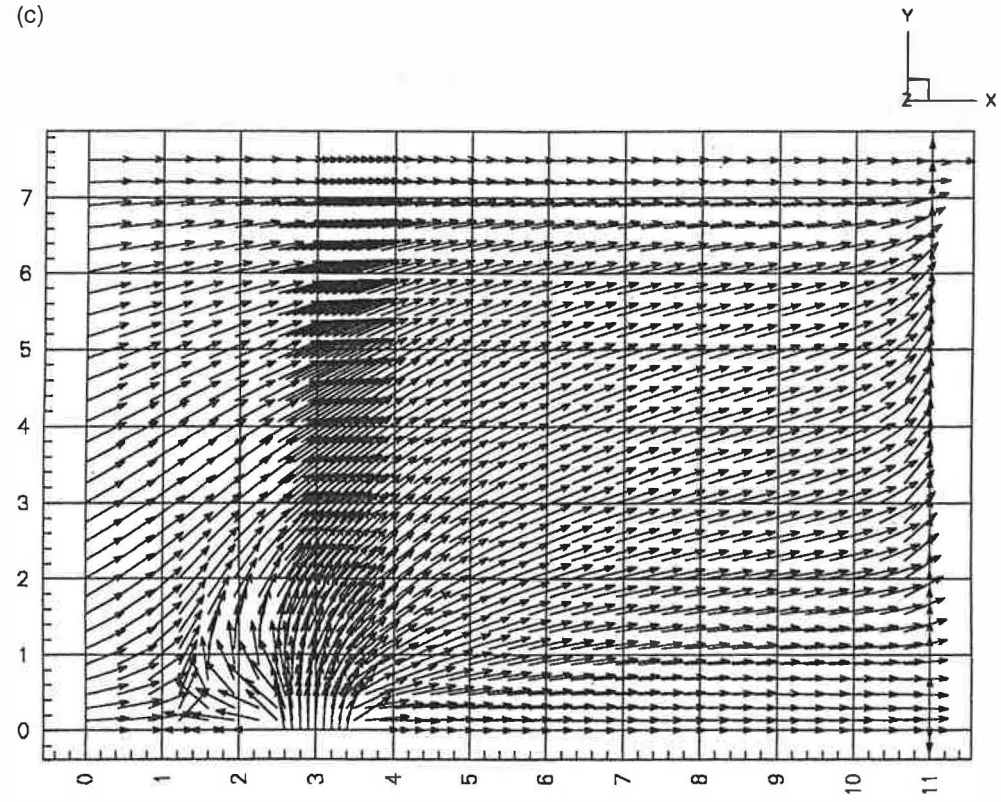

Fig. 8 (*continued*)

- x–y plane at $z = 0$

  $0 < x < X_2; \quad 0 < y < Y_1; \quad z = 0$

  This plane was treated as a plane of symmetry, i.e.:

  $\partial(UV, T, k, \epsilon, C)/\partial z = 0; \quad W = 0$

- x–y plane at $z = Z_2$

  $0 < x < X_2; \quad 0 < y < Y_1; \quad z = Z_2$

  and

- x–z plane at $y = Y_1$

  $0 < x < X_2; \quad y = Y_2; \quad 0 < z < Z_2$

  were considered to be far from the jet and had the same flow conditions as the upstream y–z plane.

- x–z plane at $y = 0$

  $0 < x < X_1; \quad 0 < z < Z_2; \quad X_1 < x < X_1 + D;$

  $Z_1 < z < Z_2; \quad X_1 + D < x < X_2; \quad 0 < z < Z_2$

  $\partial(U, W, T, k, \epsilon, C)/\partial y = 0; \quad V = 0$

  Characteristics of pollutant are present in a recent study [10].

4. Calculations

To assess the validity of flow modeling and the com puter program, a case of turbulent jet emitted no mally to a uniform free stream of homogenous flui with $V_e/U = 2$ is computed at first and compared wit previous studies [7–9]. Computations are held for th both the standard value of $c_{\epsilon 3}$ and the adopted one i this study (Fig. 2). It is seen that there is a good qual tative agreement between the results on the profi shapes and magnitudes.

Two grid distributions are used for $V_e/U_a = 8$. Fig. shows the comparison of the computed V velocity pr files at the plane of symmetry at several stations alor the stream direction. Although it indicates a differenc near the exit, the deviation of the V profiles betwee the computed results of the grid size $44 \times 30 \times 39$ an those of the fine grid $62 \times 43 \times 56$ is not significan Therefore, the results are based on the grid numbe of $44 \times 30 \times 39$. Seven of the 44 grids in x directio are ahead of the jet which is 2.5 D in length and 2 grids are downstream of the jet which is 7.5 D length. The remaining 10 grids of the 44 grids in direction is distributed over the jet exit which is D length. Similar non-uniform distributions have bee performed in y and z directions.

In the present study seven flow cases are computed to study the effect of the exit velocity and exit temperature on a jet or plume flow, subject to a uniform velocity cross flow. The jet conditions and the flow parameters of these flows are listed in Table 1 where the discharge Froude number is defined as:

$$Fr = \frac{V_e^2}{g\beta(\Delta T)D} \tag{13}$$

5. Results

Fig. 4 shows the V velocity contours and iso-concentration contours of the jet flow interacted with the cross flow on the plane of symmetry ($z = 0$). The figure illustrates the computed results for the pure momentum jet in the cross flow of unstratified fluid for $V_e/U = 8$ case. Above the exit, the jet, driven by its initial momentum, continues to move upwards. It can be seen from Fig. 4a that the turbulent shear generated by the discharge, results in efficient mixing

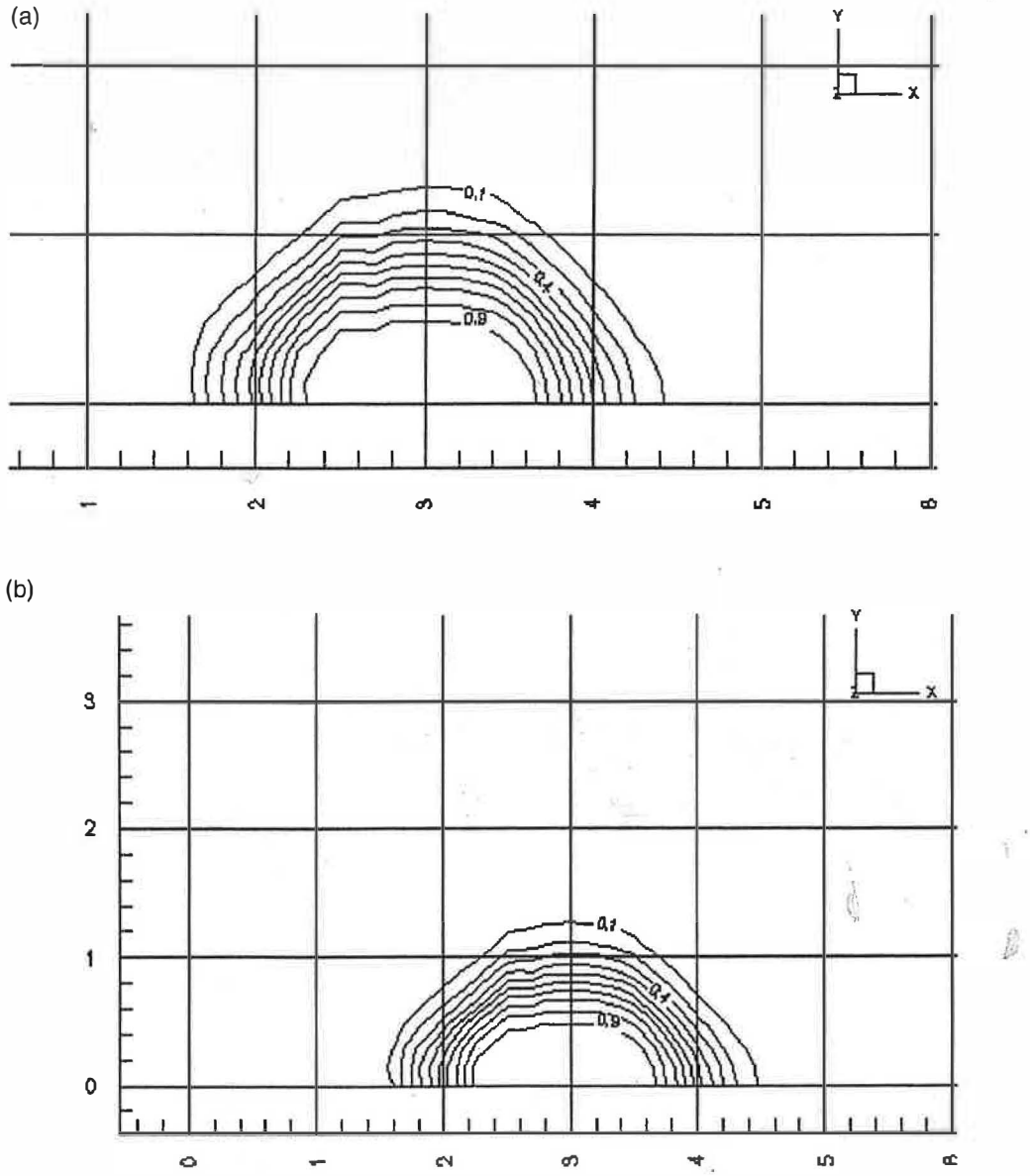

Fig. 9. The iso-concentration contours for various jet exit velocities: (a) $V_e/U = 8$ ($Fr = 13.22$); (b) $V_e/U = 4.5$ ($Fr = 3.31$); (c) $V_e/U = 2.0$ ($Fr = 0.65$); (d) $V_e/U = 1$ ($Fr = 0.16$).

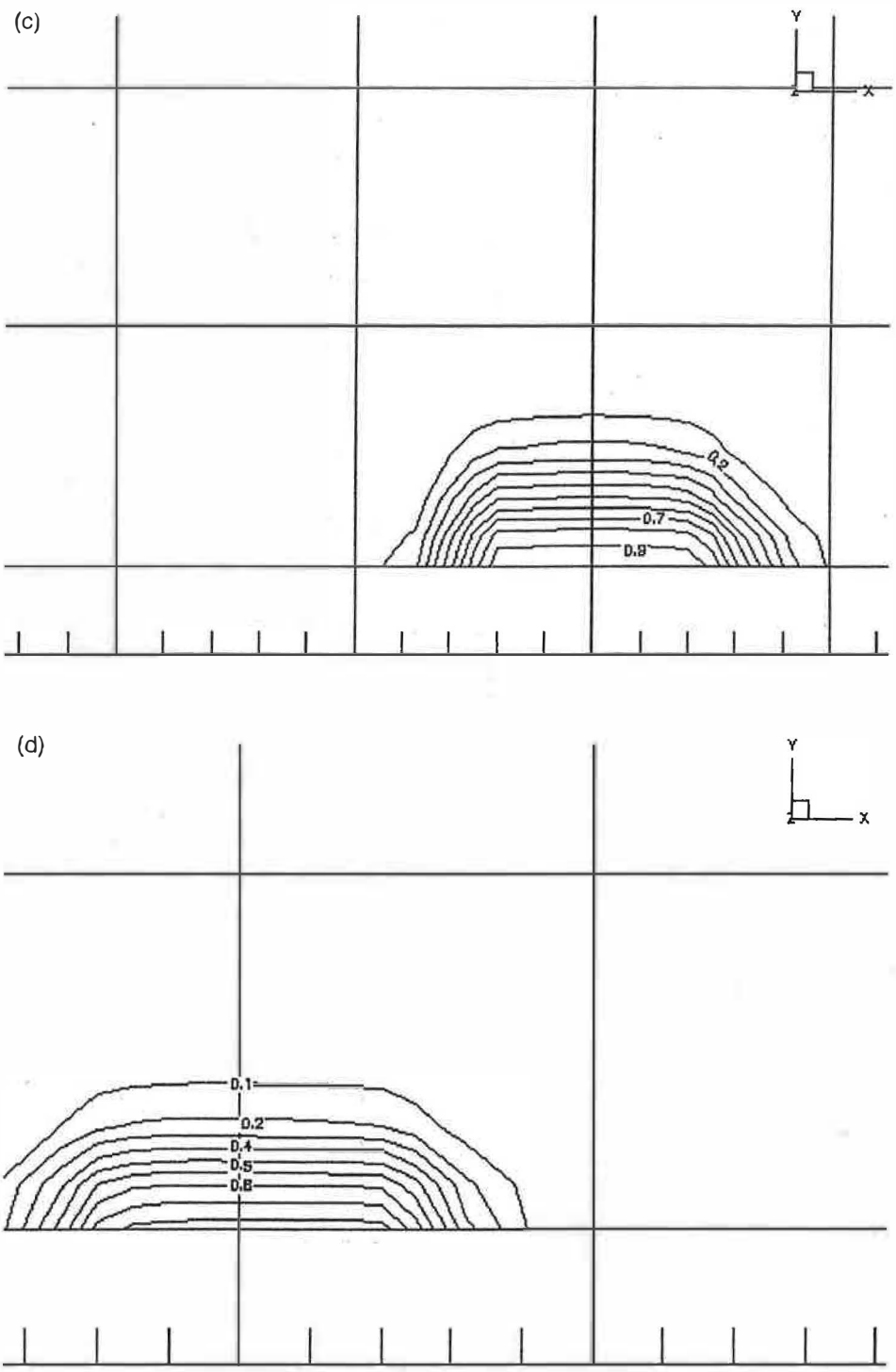

Fig. 9 (*continued*)

which rapidly reduces tracer concentrations. Fig. 4b shows the computed concentrations of the dyed jet to be reduced in the vicinity of the jet exit.

Some details of the flow near jet exit for the case $V_e/U = 18$ are illustrated by the velocity vector plots in the vertical plane in Fig. 5. This vertical section shows significant upward velocity in the lee of the j indicating convergence into the wake; this is t entrainment mechanism which brings environmen fluid into the jet (Fig. 5a). The cross stream is lift over the bent over jet. In Fig. 5b the reversed flow observed immediately behind the jet; this is consiste

with laboratory experiments, reported in literature [9], which describes the initial jet as acting like a solid cylinder around which the free stream separates and forms a vortex. As it is observed from the experimental data reported in literature [8], the flow does not recirculate. Here the reversed flow is restricted very near to the jet exit. The cross stream enters to this reversed flow region, travels upstream and is lifted by the jet. Thus, the difference between the jet and a solid obstacle inserted in the flow is that the jet interacts with the deflected flow and entrains the fluid from it.

As the ratio of the jet exit velocity to the free stream velocity decreases, the entrainment becomes weaker (Fig. 6). Increasing the ratio of the jet velocity to the

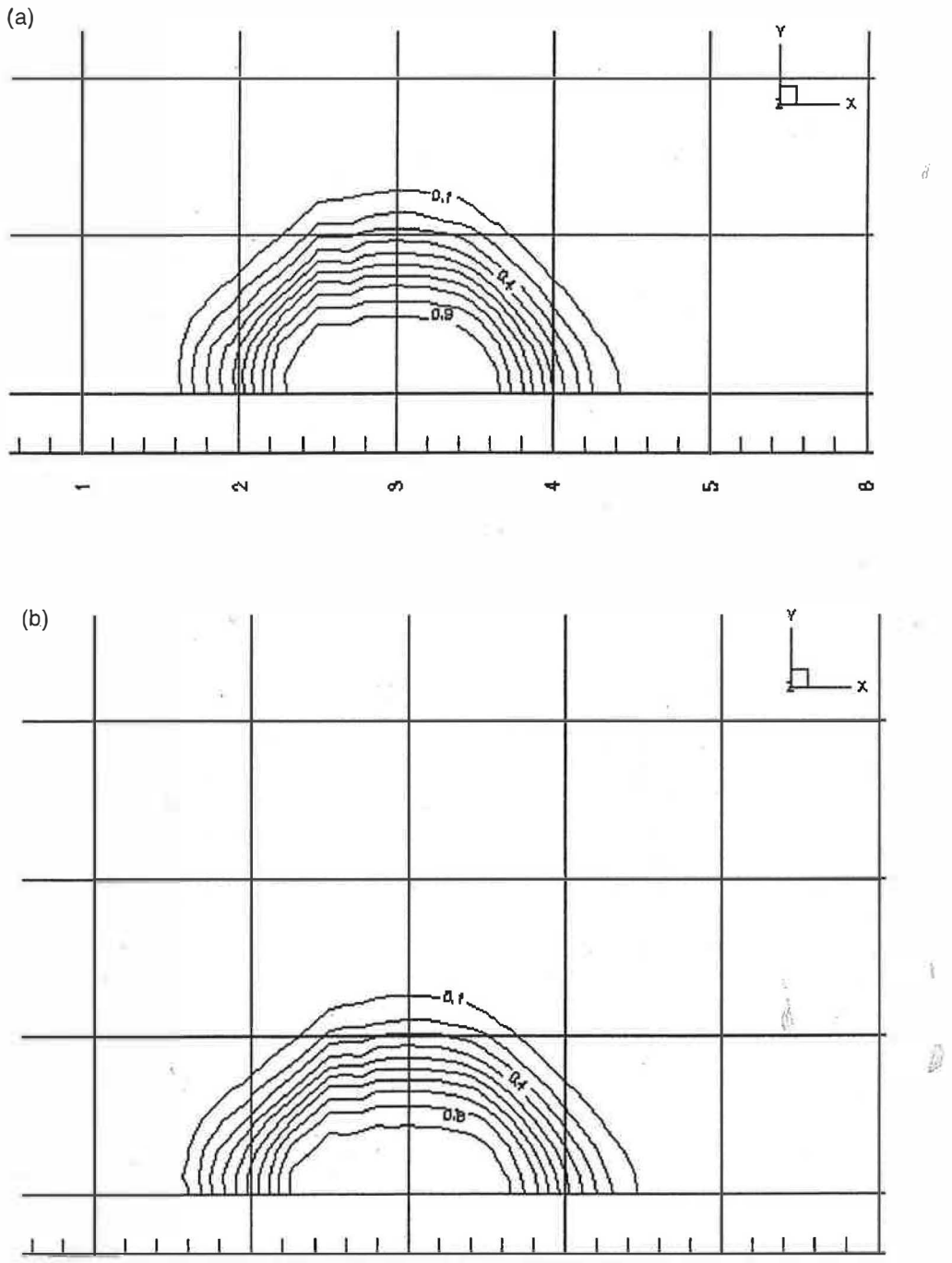

Fig. 10. The iso-concentration contours for various jet exit temperatures at constant exit velocity: (a) $T_e = 600$ K ($Fr = 13.22$); (b) $T_e = 450$ K ($Fr = 24.55$); (c) $T_e = 275$ K ($Fr = \infty$).

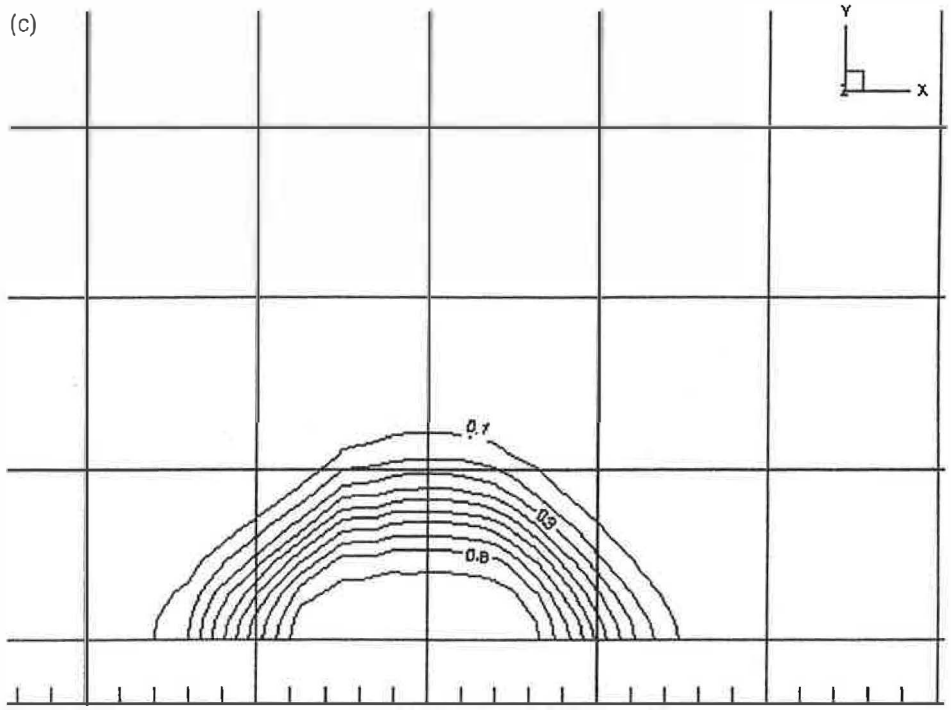

Fig. 10 (*continued*)

main stream velocity will increase the initial momentum of the jet so that the buoyant jet rises higher and mixes more rapidly with the bottom fluid.

The cross flow bends sharply over the jet and streamlines are strongly curved. The plume first behaves like a buoyant jet. The initial momentum and the buoyancy of the plume cause the jet flow to move upward.

Fig. 7 shows the decay of the reversed flow with decreasing the jet exit ratio. For lower jet exit velocities, the initial momentum of the jet is not dominant on the cross stream to form a reversed flow. When the jet is discharged with lower exit temperatures, the reversed flow is replaced by the mixing of the jet with the surrounding fluid (Fig. 8).

The effect of exit velocity and temperature on the mixing of the jet with the surrounding fluid, can also be observed from Figs. 9 and 10. The lateral location where the concentration reduces to atmospheric value is inversely proportional with the exit velocity at a constant exit temperature. However, the maximum height, where the atmospheric iso-concentration line passes through, increases with the plume rise which is proportional to the exit velocity.

6. Concluding remarks

As a turbulent jet or plume, issues vertically into a cross flow, the flow field can be viewed from two views. To the surrounding fluid, the discharged jet behaves similarly to an obstacle placed in the flow, where the windward side is the retarding region of the high pressure and while the lee side is the low pressure wake region. To the jet flow, the horizontal momentum of the cross flow and the shear layer and wake entrainment lead to the deflection of the jet in the cross flow direction, mixing with the surrounding fluid.

Higher jet exit velocities effect the reversed flow and entrainment mechanism of the jet and the major effect of decreasing the discharge velocity is to limit the vertical rise of a buoyant jet and to restrict the dilution compared to similar flows with higher exit velocities. With lower discharge velocities, there is a strong interaction between the jet and the cross flow in the jet exit. Exit temperature, on the other hand, does not effect the lateral and vertical coordinates of the plume formation, but it decreases, concentration reduces more rapidly towards the inside of the stack. Thus, the mixing process inside the reversed flow region of the higher velocities and higher temperatures grows up.

It should be noted that the formations of secondary and third pairs of vortices are not induced in this study since the ambient has been assumed as unstratified.

From the computational point of the view it is concluded that the reduction of the value of $c_{\epsilon 3}$ led to an improved prediction for the velocity field. The presen

solution indicates that further downstream of the jet, the flow assumes a boundary layer character. A more general model relation would require introducing a functional dependence of the coefficient of buoyancy in the structure of turbulence field.

References

[1] Jin Y. Experimental study of plume rise in a stably stratified environment ASHRAE Transactions. Part 2. 1991;340.

[2] Petersen RL, Ratcliff M. An objective approach to laboratory stack design. ASHRAE Transactions. Part 2. 1991;553.

[3] Schulman LL, Scire JJ. The effect of stack height, exhaust speed and wind direction on concentrations from a rooftop stack. ASHRAE Transactions. Part 2. 1991;573.

[4] White BR. Wind tunnel study of atmospheric dispersion of near field exhaust from a stack. ASHRAE Transactions Part 2. 1991;589.

[5] Hossain MS, Rodi W. A turbulence model for buoyant flows and its aplication to vertical buoyant jets. In: Rodi W, editor. Turbulent buoyant jets and plumes, HMT, vol. 6. Oxford: Pergamon Press, 1982. p. 121–78.

[6] Bergstrom DJ, Strong AB, Stubley GD. Algebraic stress model prediction of a plane vertical plume. Numerical Heat Transfer, Part A 1990;18:263–81.

[7] Hwang RR, Chiang TP. Numerical simulation of vertical forced plume in a crossflow of stably stratified fluid. Journal of Fluids Engineering 1995;117:696–705.

[8] Andreopoulos J, Rodi W. Experimental investigation of jets in a crossflow. J Fluid Mech 1984;138:93–127.

[9] Sykes RI, Lewellen WS, Parker SF. On the vorticity dynamics of a turbulent jet in a crossflow. J Fluid Mechanics 1986; 168:393–413.

[10] Özdoğan S, Uygur S, Eğrican N. Formation and dispersion of toxic combustion by-products from small scale combustion systems. Energy — The International Journal 1997;22(7):681–92.